A METHOD FOR COARSE SEGMENTATION OF PATHOLOGICAL LUNGS ON CT IMAGES USING RIBCAGE

V.A. Liauchuk, E.V. Snezhko

United Institute of Informatics Problems, Minsk, Belarus

e-mail: vitali.liauchuk@gmail.com

A method is proposed for coarse segmentation of lung regions on CT images in the presence of lung pathology. The goal of the approach is to coarsely extract lung regions using only the skeleton (basically ribcage), thus eliminating most of the difficulties of pathological lung segmentation. The method is based on a model of elastic deformable surface, which tends to iteratively fit the ribcage. The method demonstrates good results in the task of segmenting images of lungs, strongly affected by a disease, what is important in terms of automated computer analysis of lung diseases.

Introduction

The problem of extraction of regions of interest is usually considered as a preprocessing step in various image analysis algorithms. In this context the task of lung segmentation on three-dimensional computed tomography (CT) images is of great importance in medical image analysis. A lot of work was done in order to achieve high-performance robust solutions for extracting lung regions on CT images [1 – 3]. In the case of healthy patients, lung segmentation on CT appears to be not so difficult due to large intensity differences between lung regions and surrounding tissue. Thus adaptive thresholding followed by morphological operations may lead to reasonable segmentation quality.

However in the case of pathology (e.g., pneumonia, fibrosis, tuberculosis, etc.) the task of extraction of correct lung regions becomes challenging. Being applied to images with pathology, conventional methods usually leave some lesion parts out of segmentation. Various approaches were developed in order to overcome the disadvantages of traditional lung segmentation methods [4 – 8]. In [4] the authors propose the segmentation method based on elastic registration of CT lung atlas to a target image of pathological lungs. In [7] and [8] the ribcage shape is used to set the initial iteration of the corresponding dynamic model (Snake Model and Active Shape respectively) which is used for further lung segmentation. Utilizing ribcage within the lung extraction process makes the corresponding algorithm more robust because ribcage is usually not affected by diseases and it can be easily extracted from images. In this regard, using ribcage for lung segmentation on CT images looks promising.

The main idea of the method proposed with this paper is to examine how well pathological lungs on CT images can be extracted using only the information about skeleton structure. Considering only high-density structures with intensity > 450 Hounsfield Units (HU) we can automatically avoid most of the challenges caused by the presence of pathology. In some cases lung disease leads to high-density structures inside the lung (e.g., calcifications). However, the proposed method appears to be insensitive to these minor changes of image structure. Thus, the goal of our method is to perform coarse segmentation of pathological lungs on CT images using only information on dense structures present on images (ribcage, spine and other bones). Focusing on analysis of lung pathology here we do not claim extraction of accurate lung regions. Instead we allow the final segmentation to capture some inner organs (trachea, heart, parts of stomach), expecting the method to segment most of the lesions.

In this paper, the segmentation is performed with use of energy-minimizing restricted active surface model similar to active contour. The shape is initialized near the ribcage and its evolution is guided by cost function considering internal and external energy. In contrast to conventional active contour, here external energy is defined by averaged bones intensity rather than gradient magnitude. The method is tested on CT images of pathological lungs taken from publically available image database [9].

1. Materials

The dataset used for testing our method consisted of 149 CT chest scans of tuberculosis patients. Three-dimensional CT images consisted of axial slices of size 512×512 pixels. The number of slices varied from 100 to 250 depending on scanning parameters and slice thickness (2.5 mm or 1.25 mm). In addition to original images (Fig. 1a) for each case three versions of segmentation were available: automated segmentation of lung regions based on adaptive thresholding and morphological operations (Fig. 1b), semi-automated lung segmentation (Fig. 1c) and manual segmentation of lesions and surrounding tissue (Fig. 1d). Semi-automated segmentation, which is considered as ground truth with this study, consisted of two major steps: threshold-based automated segmentation followed by manual corrections of segmentation mistakes.

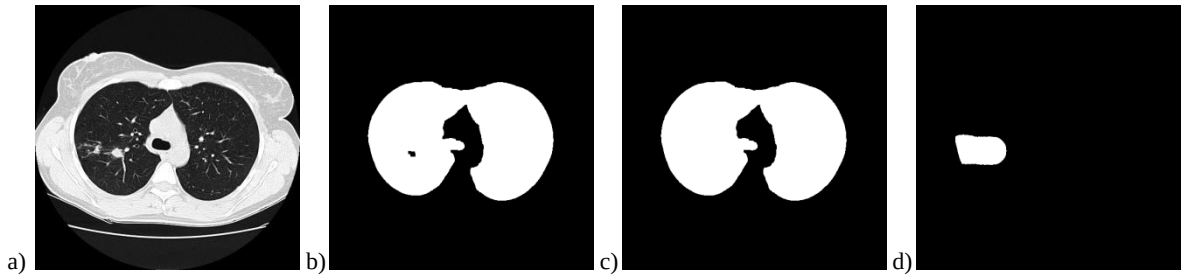

Fig. 1. Example slices of original image (a) and its segmented versions:
automated threshold-based (b), semi-automated (c) and manual lesion segmentation (d)

2. Methods

In this work, a restricted deformable model is used for coarse segmentation of lungs using ribcage. The model incorporates a deformable surface represented by a set of vertices and edges. The evolution (deformation) of the surface is controlled by a cost function. By saying "restricted" we mean that each vertex is allowed to move towards only the predefined directions – along the line connecting the considered vertex and a reference point called "center", which is not necessarily the geometric center of image (Fig. 2a). Thus, each vertex has only one degree of freedom instead of three. This restriction makes our model more stable and easy to control. However, it goes only under assumption that the shape of the region of interest to be extracted is simple enough.

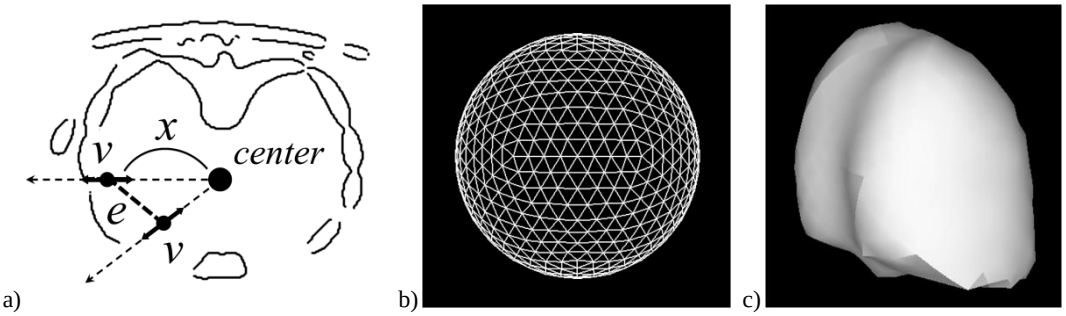

Fig. 2. Deformable surface: scheme of deformation (a),
homogeneous spherical surface (b), deformed surface representing segmented lungs (d)

The proposed segmentation algorithm includes the following major steps:

- extracting bones, image preparation;
- generating homogeneous spherical surface;
- setting the initial iteration;
- iterative deformation of the surface;
- converting the final surface shape to raster mask.

Thus the final shape of the surface which best fits the ribcage while remaining smooth enough corresponds to the extracted lung region.

Image preparation step implies the extraction of high-density structures (ribcage, spine and other dense objects) present on the image and calculating the map of so called "closeness" to the ribcage for every image voxel. This is done by performing the following simple operations: binarizing the image using fixed threshold (450 HU), Gaussian smoothing (with STD = 6.5 mm), limiting the obtained values (to somehow equalize thick and thin bones' contribution) and another Gaussian smoothing (smoothed field is suitable for gradient-descent minimization method). Applying the threshold of 450 HU almost completely eliminates the effects, appearing in the case of lung pathology (except for calcifications). With this preliminary study we didn't try to remove any undesired high-density objects like bench or calcifications, what makes our current task a bit more difficult.

The shape of the active surface used for segmentation originates from *homogeneous sphere surface*, i.e. when not deformed all faces (triangles) of the surface should be equal. For this purpose we utilize the method of quasiregular tesselation of a sphere proposed in [10]. Thus, all the edges of the surface have almost the same length what makes our surface isotropic. In our case the obtained sphere surface contained 642 vertices connected by 1920 edges, which formed 1280 faces (Fig. 2b).

The cost-function to be minimized by the deformation process includes two terms which consider internal (elasticity) and external ("closeness" to ribcage) moving forces:

$$f(x) = f_{ex}(x) + \alpha \cdot f_{in}(x) = -\sum_{i=1}^{n} C(v_i(x)) + \alpha \cdot \sum_{j=1}^{m} \left\| e_j(x) \right\|^2 , \quad (1)$$

where f_{in} and f_{ex} denote terms, corresponding to internal and external forces respectively, α – weighting coefficient, x is a vector of n arguments which control the positions of vertices, n and m being the numbers of vertices and edges respectively, v_i represents i-th vertice, e_j represents j-th edge, $C(v)$ denotes the value of closeness to ribcage and $\|e\|^2$ is the squared length of edge. Thus, our surface tends to get closer to the ribcage with minimum tension.

The *initial iteration* (initial surface) is set up in two steps. On the first step we coarsely find high-density structures by minimizing cost-function for each vertex separately with $\alpha = 0$ (eliminating the cost-function elasticity term). Then the coefficient α is set to the needed positive value and the procedure is repeated. The form of cost-function used with this study allows us to draw partial derivatives $\frac{\partial f}{\partial x_i}$, therefore finding x which minimizes the cost-function was performed via gradient descend method. Finally, image voxels which correspond to the interior of the deformed surface constitute the region of interest, i.e. coarsely segmented lung region. Example of the deformed surface is shown in Fig. 2c.

3. Experimental results

The lung segmentation method proposed was tested on the whole dataset of 149 CT scans. In different cases lungs were affected by disease at different extent, from small nodules to lung collapse and large fibrosis regions. The performance of our method was compared with an automated method based on thresholding and morphological operations (Fig. 1b) by means of calculating the following two indices. The first one is segmentation agreement which is helpful for general assessing of segmentation quality:

$$SA = \frac{2\left|\Omega \bigcap \Theta\right|}{\left|\Omega\right| + \left|\Theta\right|}, \quad (2)$$

where Ω corresponds to tested segmentation, Θ represents segmentation ground truth (semi-automated segmentation), $\bigcap$ is intersection and $|\bullet|$ denotes regions size. The other index is important in terms of analysis of lung pathology and estimates the size of lesion part left outside of segmented region:

$$Miss = \frac{\left|\overline{\Omega} \bigcap \Delta\right|}{\left|\Theta\right|}, \quad (3)$$

where Δ corresponds to manually segmented lesions (Fig. 2d) and $\overline{\Omega}$ is exterior of Ω.

Fig. 3 demonstrates some segmentation results of the proposed method in comparison with threshold-based approach. Here we see that even significant changes in lung anatomy caused by diseases do not influence the segmentation results. However the method includes some mediastinum into the segmentation. Thus, segmentation agreement between the proposed method and ground truth segmentation is rather low (average 0.76 in contrast to 0.98 for threshold-based method).

Fig. 4 shows that traditional threshold-based method often leaves significant parts of affected lung regions outside of segmentation. With this respect the proposed method performs significantly better (better in 87 cases out of 149), what is important for automated analysis of pathological lung images. Average lesion miss index for our method is 0.0038 in contrast to 0.061 for threshold-based one.

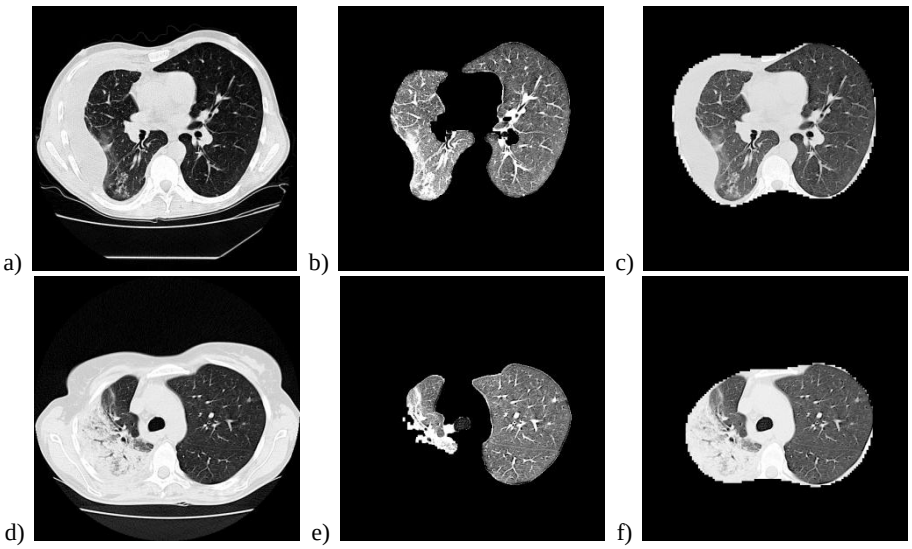

Fig. 3. Slices of original images (a, d), their threshold-based segmentation (b, e) and segmentation by the proposed method (c, f)

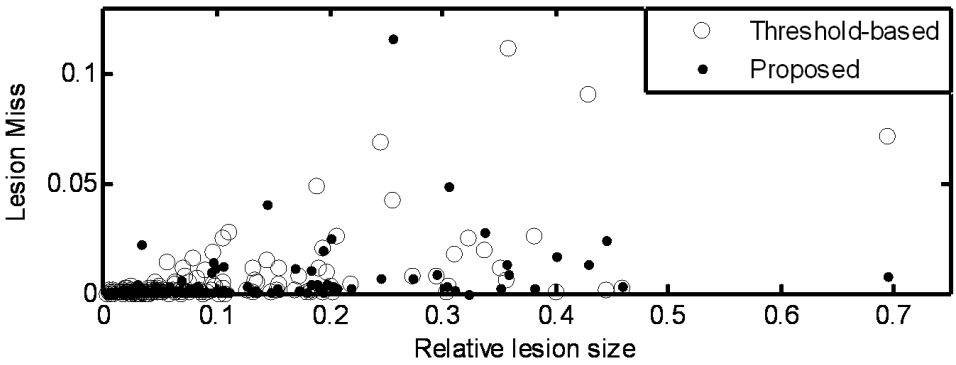

Fig. 4. The performance comparison of lung segmentation methods

Conclusion

The approach for pathological lung segmentation suggested with this study may be considered as a promising tool, useful for computer analysis of lung diseases. The segmentation result, produced by the method, is almost not influenced by any pathology.

However the method has disadvantages and its performance needs to be improved.

Acknowledgments. This work was partly funded by the National Institute of Allergy and Infectious Diseases, National Institutes of Health, USA through the CRDF project BOB1-31120-MK-13**.**

References

1. Armato, S.G. Automated lung segmentation for thoracic CT / S.G. Armato, W.F. Sensakovic // Acad. Radiol. – 2004. – Vol. 11(9). – P. 1011–1021.

2. Automated lung segmentation in X-ray computed tomography / J.K. Leader [et al.] // Acad. Radiol. – 2003. – Vol. 10(11). – P. 1224–1236.

3. Hu, S. Automatic lung segmentation for accurate quantitation of volumetric X-ray CT image / S. Hu, E.A. Hoffman, J.M. Reinhardt // IEEE Trans. Med. Imag. – 2001. – Vol. 20(6). – P. 490–498.

4. Sluimer, I. Toward automated segmentation of the pathological lung in CT / I. Sluimer, M. Prokop, B. van Ginneken // IEEE Trans. Med. Imag. – 2005. – Vol. 24(8). – P. 1025–1038.

5. Automatic segmentation of lung parenchyma in the presence of diseases based on curvature of ribs / M.N. Prasad [et al.] // Acad. Radiol. – 2008. – Vol. 15(9). – P. 1173–1180.

6. Wang, J. Automated segmentation of lungs with severe interstitial lung disease in CT / J. Wang, Q. Li, F. Li // Medical Physics. – 2009. – Vol. 36(10). – P. 4592–4599.

7. Meng, L. A New Lung Segmentation Algorithm for Pathological CT Images / L. Meng, H. Zhao // Proc. of Inter. joint conf. on Computational Sciences and Optimization. – Sanya, 2009. – P. 847–850.

8. Robust Active Shape Model Based Lung Segmentation in CT Scans / S. Sun, C. Bauer, R. Beichel // Proc. of the Fourth International Workshop on Pulmonary Image Analysis. – 2011. – P. 213–223.

9. Belarus Tuberculosis Portal [Electronic resource]: http://tuberculosis.by – Last visited: 21.01.2014.

10. Petrokovets, E. Quasiregular Tesselation of Arbitrary Sphere / E. Petrokovets, V. Kovalev // Proc. of the Fifth International Conference on Pattern Recognition and Information Processing (PRIP'99). – 1999. –Vol. 1. – P. 243–248.